SUPPLEMENT 1: Physical Oceanographic Model Validation

Shanks (2013) observed that more megalopae were caught in a light trap fished in Coos Bay Oregon during a negative phase PDO and hypothesized that this was because more water was transported into the California Current from the West Wind Drift during negative phase PDO's increasing the flow in the Current, which transported more larvae south to central Oregon. For each PDO phase, we generated a wintertime average of alongshore flow off of the continental shelf in order to compare variations in alongshore flow. On average flow was more southward during negative phase PDO years than positive phase PDO years (Fig. S1).

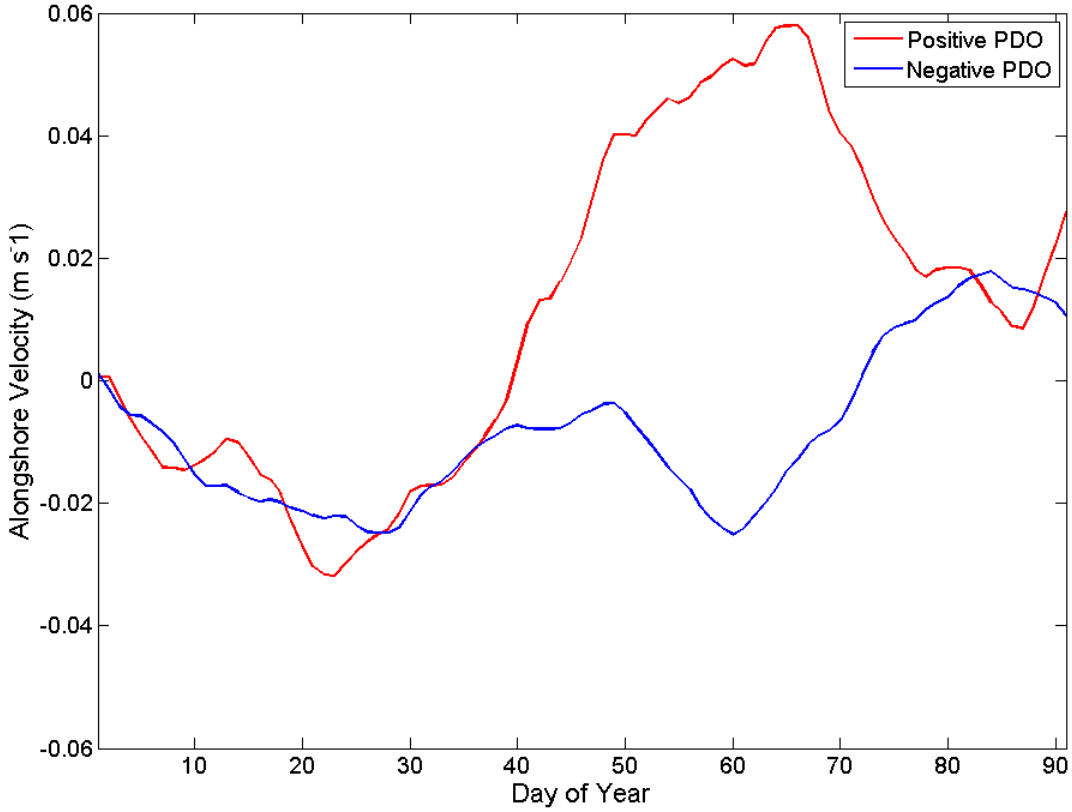

Fig S1. Average alongshore flow off of the continental shelf during winter months during positive (red) and negative (blue) PDO phases. Negative values denote southward flow and positive values denote northward flow.

Shanks et al. (2007, 2010, 2013) also demonstrated that more Dungeness crab megalopae were caught when the day of the spring transition was earlier in the year. We calculated the day of the spring transition for each model year, as the day the flow along the continental shelf changed from being predominately from the south to predominately from the north. The date of the observed spring transition was correlated with the modeled day. Overall the model did a good job of representing the day of the spring transition (Fig. S2).

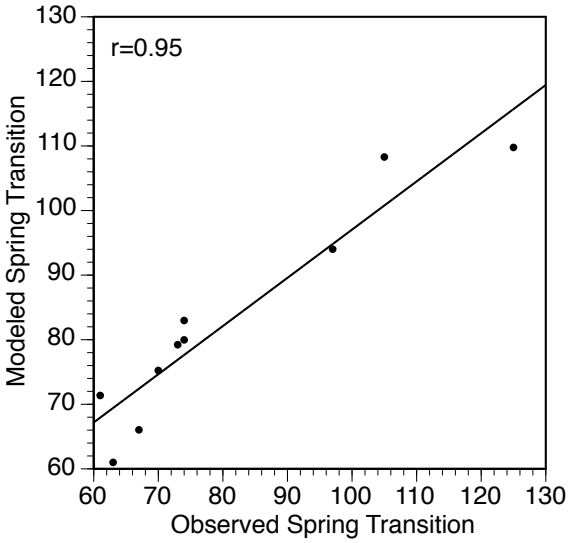

Fig S2. Observed versus modeled day of the year of the spring transition.

SUPPLEMENT 2. LARVAL PRODUCTION AND MORTALITY

Production

The Dungeness crab fishery is managed using a 3-S management structure; a technique that regulates the size of crabs harvested, sex of crabs harvested (male) and the season when crabs are harvested (Rasmuson 2013). The 3-S management structure results in the annual extraction of nearly all 4-yr old male crabs. This allows us to relatively accurately predict 1) the number of females in the population and, because essentially all females are mated each year, 2) the number of larvae that are released annually. Our model uses the following assumptions from (McKelvey et al. 1980). First, that the sex ratio between males and females is 50:50. Second, that female crabs begin reproducing at age 2 and are capable of reproducing until they are 8-yr old. Third, we assume that 78% of the population survives each year. Fourth, all females mate successfully (Hankin & Oh 2004, Dunn & Shanks 2012). Finally, we assume that on average a 4-yr old crab weighs 0.9 kg (2 lbs).

In order to calculate annual larval production, we first compiled total annual catch (in lbs) in California, Oregon and Washington from 1981-2014 (PSMFC). Since our hydrodynamic model was run from 2000-2001 and 2006-2013, we needed catch data for 2015-2017 to calculate larval production for the final years our model was run. Since these fishery years had not occurred, we fit the catch data from 1981-2014 with a first order autoregressive integrated moving average (ARIMA). Using this model, we conducted 100,000 simulations to predict commercial catch from 2015-2017. We calculated a mean of the 100,000 simulations for each year from 2015-2017. We used these data to calculate larval production similar to the methods used by Shanks & Roegner (2007).

We calculated the number of 4-yr old females using:

$$F_{yr} = C_{yr} \qquad \text{S.1}$$

where F_{yr} is the number of 4 year old females and C_{yr} is the total commercial catch in a given year. Then we calculate the number of 2 and 3 year old females using:

$$F_{yr+k} = C_{yr+k} + 0.12k(C_{yr+k}),\ \text{for k=1, 2} \quad \text{S.2}$$

Where k is scaling factor to adjust for the catch years following C_{yr} and $0.12k$ adjusts C_{yr} to account for the larger population size due to fewer years of annual mortality. We calculate the number of 5-8 yr old female crabs using:

$$F_{yr-k} = (C_{yr-k})0.78^{k},\ \text{for k=1, 2, 3, 4} \quad \text{S.3}$$

Where again k is a scaling factor used to adjust for catch years preceding C_{yr} and 0.78^{k} decreases the population size based on a fixed mortality rate (0.78) and the number of years since the commercial catch, k. Thus, using equations S.1-3, the total number of female crabs (age 2-8) in any given year can be expressed as:

$$F_{yr} = \left(\sum_{k=1}^{2} F_{yr+k}\right) + F_{yr} + \left(\sum_{k=1}^{4} F_{yr-k}\right) \quad \text{S.4}$$

Where F_{yr} is the total number of female crabs that produced larvae in a given year. If we assume each female releases approximately $2*10^{9}$ larvae (Botsford & Wickham 1978) then the total number of larvae produced is calculated as:

$$L_{yr} = F_{yr}(2*10^{9}) \quad \text{S.5}$$

Where L_{yr} is the annual total number of larvae released into the California Current each year and F_{yr} is the total number of females calculated in equation A.5. From these calculations it is evident that the total amount of larvae released into the California Current is not equal between years, ranging from a low of ~$2*10^{13}$ in 1984 to a high of $7.7*10^{13}$ in 2005 (Fig. S3).

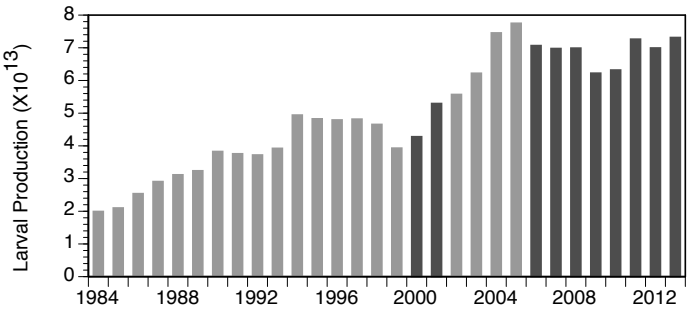

Fig S3. Number of larvae produced each year from 1984-2013. Darker gray bars denote years we modeled larval dispersal.

For our model, ideally we would have liked to alter the number of particles released each year to match the number of larvae produced that year, however, the large number of larvae released each year made this computationally prohibitive. Thus, we scaled the annual larval production on a scale of 0 -1 using:

$$SL_{yr} = \frac{\left(L_{yr} - \min(L_{yr})\right)}{\left(\max(L_{yr}) - \min(L_{yr})\right)} \quad \text{S.6}$$

Where SL_{yr} is the scaling factor for each year, $min(L_{yr})$ is the minimum value of larval production from 1984-2013 and $max(L_{yr})$ is the maximum value of larval production over this period. This generated a scaling value that we could multiple the initial super individuals to better include potential impacts of larval production in our model (Fig. S4). Super individuals are a technique where each particle in the Lagrangian model represents a greater number of individuals (in our

case 10^6) which allows researchers to include mortality in the model while maintaining a computationally efficient model. Although the values are scaled from 0-1, none of the years that we modeled (2000-2001 & 2006-2013) were scaled to a zero.

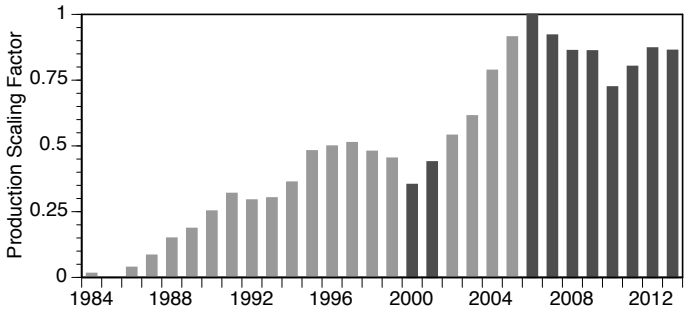

Fig S4. Scaling factor for larval production from 1984-2013. Darker gray bars denote years we modeled larval dispersal.

Mortality

In addition to altering the number of larvae produced for each model year, we wanted to include a measure of mortality rate in our model as this has been shown to profoundly impact model results (Cowen et al. 2000). Mortality rates of marine larvae are notoriously difficult to measure (Rumrill 1990), especially for widely dispersing species like Dungeness crabs. Using the number of larvae produced each year (L_{yr}) we were able to calculate the number of settlers using:

$$Nt_{yr} = N0_{yr} e^{-M*t} \quad \text{S.7}$$

where Nt_{yr} is the total number of settlers in a given year, t is the amount of time from larval release to settlement, M is mortality rate and $N0_{yr}$ is the number of larvae released each year which can be assumed to be:

$$L_{yr} = N0_{yr} \quad \text{S.8}$$

To calculate the number of settlers, we assumed t was equal to the day of the year of the spring transition (St_{yr}), obtained from the "Wind stress, cumulative wind stress, and spring transition dates: data products for Oregon upwelling-related research" website (Pierce & Barth), since this is the first day that large numbers of Dungeness megalopae are often caught. Essentially this assumes that the pelagic larval duration is from January 1 until the day of the year of the spring transition, likely a large underestimation since megalopae are caught in the light trap for upwards of 100 days following the spring transition. Thus, by substituting equation S.8 into S.7 and St_{yr} for t we can calculate larval settlement over a range of mortality rates as:

$$Nt_{yr} = L_{yr} e^{-M*St_{yr}}, \text{ for m} = 0.01, 0.02, ..., 0.25 \quad \text{S.9}$$

To assess which mortality rate best reflects the population, we calculated the number of settlers in a year (Nt_{yr}) using equation A.2 and a k value (scaling factor for catch data) of 4. We then could determine a range of mortality rates for both the maximum and minimum number of settlers.

Total number of settlers dropped quickly as mortality rate increased (Fig. S5). From 1984-2013 the maximum number of settlers would have been ~10^{13} individuals, which would have occurred over a range of mortality rates from 0.02-0.05. The minimum number of settlers would have been ~10^{12} individuals which would have occurred over a range of mortality rates from 0.04-0.08.

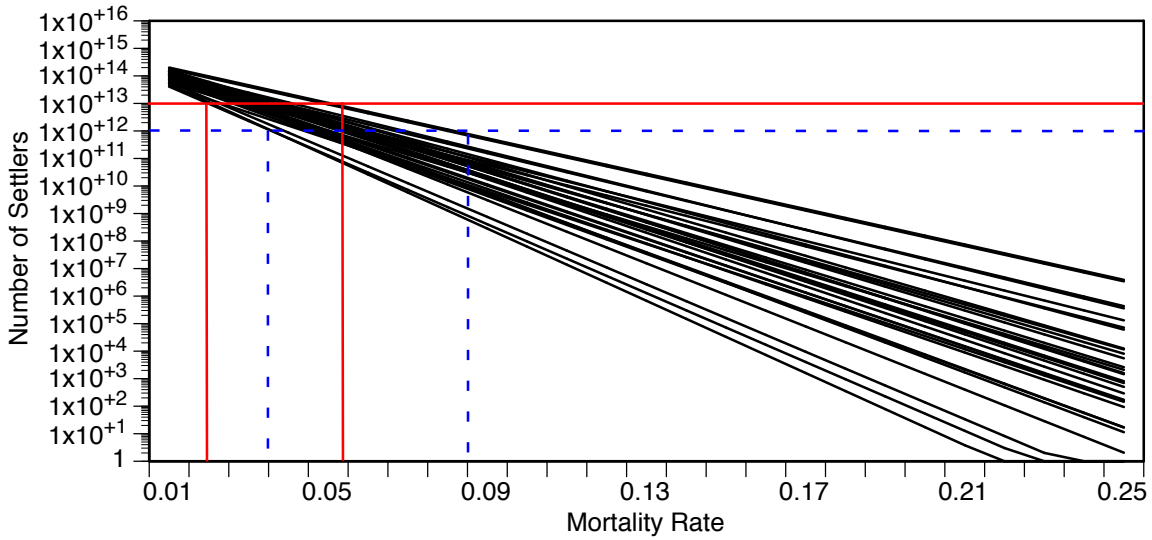

Fig S5. Total number of settlers versus mortality rate based on annual larval production values from 1984-2013. The horizontal lines denote the calculated maximum (red solid line) and minimum (blue dashed line) settlement rates. Vertical lines denote the mortality rate range for the calculated maximum (red solid line) and minimum (blue dashed line) settlement rates. Vertical line color corresponds with horizontal line color.

Larval production values calculated from commercial catch, suggest that the average daily mortality rate for Dungeness crab larvae falls between 0.02-0.08 d^{-1}. In order to further define an average mortality rate, we used data from Shanks et al. (2010) where they reported an average density of newly settled Dungeness crabs of 175 crabs m^{-2}. First, we assumed that crab settlement density was equal across the continental shelf. Using bathymetry data we calculated the shelf area (*SA*) in ranges from 0-50, 0-75, 0-100 and 0-200 m (Association). Then we could calculate the total density of juvenile crabs that settled on the continental shelf

$$\sum Dens = SA * 175 \qquad \text{S.10}$$

The above assumptions likely overestimate the total number of settlers. However, sensitivity analyses showed that a reduction of shelf area by as much as 75% had no effect on mortality rate. We can manipulate equation A.9 to solve for mortality rate:

$$M_{yr} = \ln\left(\frac{L_{yr}}{Nt_{yr}}\right) ST_{yr}^{-1} \qquad \text{S.11}$$

and if we assume:

$$\sum Dens = Nt_{yr} \qquad \text{S.12}$$

we can then calculate the mortality rate for each of the 30-years of catch data as:

$$M_{yr} = \ln\left(\frac{L_{yr}}{\sum Dens}\right) ST_{yr}^{-1} \qquad \text{S.13}$$

We see that mortality rates between 0.02-0.03 result in the settlement density most similar to that reported in Shanks et al. (2010) (Fig. S6). Further, on average, mortality rate ranges from 0.023-0.028 depending on the amount of shelf area used to calculate settlement. Thus, we used a mortality rate of 0.025 for our model. We conducted sensitivity analyses for rates as high as 0.08 and found little difference in the model results. These values are lower than those historically proposed for Dungeness crab but are very similar to those determined from more recent in depth observational and modeling studies of larval mortality (Hobbs and Botsford 1992).

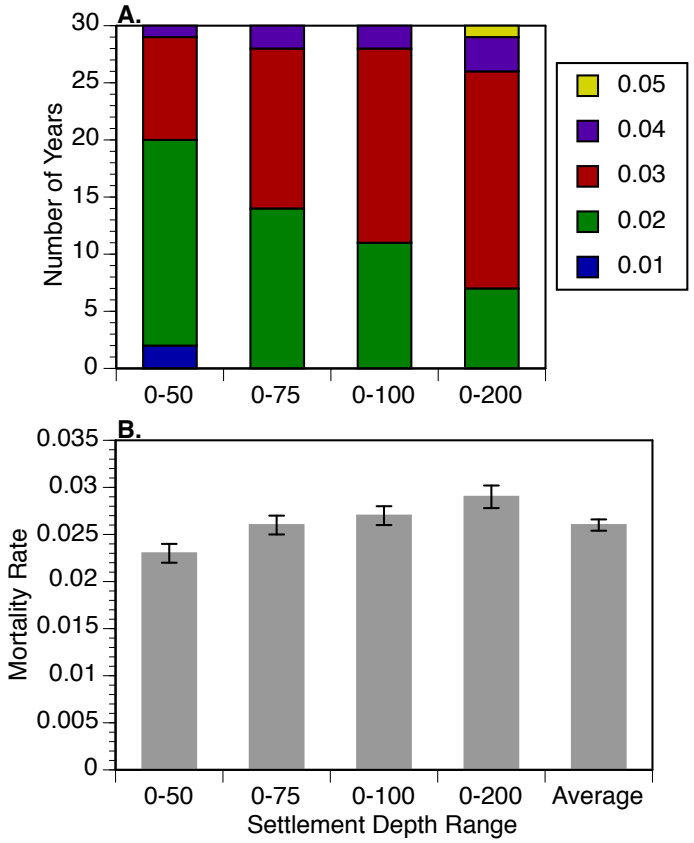

Fig S6. Number of years where each mortality rate was closest to observed settlement data with (A) and average mortality rate (B) versus settlement depth range. Colors in (A) denote mortality rates (0.01 – 0.05). Bars (B) are averages calculated based on the number of years from plot A. Bars denote ± 1 SE.

SUPPLEMENT 3: COMPARISON AND VALIDATION OF MIGRATORY BEHAVIOR

The depth Dungeness crab zoeae and megalopae occupy during the day is not well known and thus we simulated two different migration depth scenarios: shallow and deep. For the shallow migration depth simulations, depths were chosen based on migration depths suggested in the literature (Table S1; Jamieson & Phillips 1988, Hobbs & Botsford 1992). For the deep migration simulations, the zoeae and megalopae resided near the bottom during the day (Table S1). These two simulations were chosen based on much more extensive simulation modeling and validation (Rasmuson 2015) and *in situ* observations (Rothlisberg & Pearcy 1976, Reilly 1983). Both simulations were only conducted for 2001 (positive phase PDO year) and 2010 (negative phase PDO year). All other parameters were those described in the primary manuscript.

Table S1. Depth and swimming speed parameters for the shallow and deep simulations. Swimming speeds denote the speed that larvae moved vertically in the water column and values are from laboratory and *in situ* studies (Gaumer 1971, Rasmuson & Shanks 2014). Depths denote the depth larvae occupied during the day. Shallow depths are based on observational findings (Jamieson & Phillips 1988, Hobbs & Botsford 1992). Deep simulation depths are based on additional observations and modeling studies (Rothlisberg & Pearcy 1976, Reilly 1983, Rasmuson 2015). Off shelf is defined as seaward of the 200 m isobaths and on shelf is defined as shoreward of the 200 m isobaths. mab- meters above bottom

Stage	Swimming Speed (cm s^{-1})	Shallow Migration Simulation Depth	Deep Migration Simulation Depth
Zoeae I	1	20 m	1 mab
Zoeae II	1	20 m	1 mab
Zoeae III	1.5	20 m	1 mab
Zoeae IV	1.5	80 m	1 mab
Zoeae V	1.5	80 m	1 mab
Megalopae (Off shelf)	10	300 m	1 mab
Megalopae (On Shelf)	NA	0 m	0 m

From ~ April 1- September 30 of the years 2000-2001 and 2006-2013 we monitored the daily catch of Dungeness crab megalopae to a light trap operated in Coos Bay, Oregon. Each day all of the megalopae caught in the light trap were enumerated using a dissecting microscope. If the total number of individuals was >2000, the number of individuals was determined by weight of the sample (Shanks & Roegner 2007, Shanks et al. 2010). We used the time series from the light trap and compared it to the time series of settlers within 10 km of Coos Bay from the model. The time series of the light trap data were correlated with both the shallow and deep migration simulations in 2001 and 2010 in order to assess which simulations should be carried out going forward. The model that was most strongly correlated with the light trap data was considered the better fit model and simulations of additional years were conducted using the parameters of the best correlated simulation.

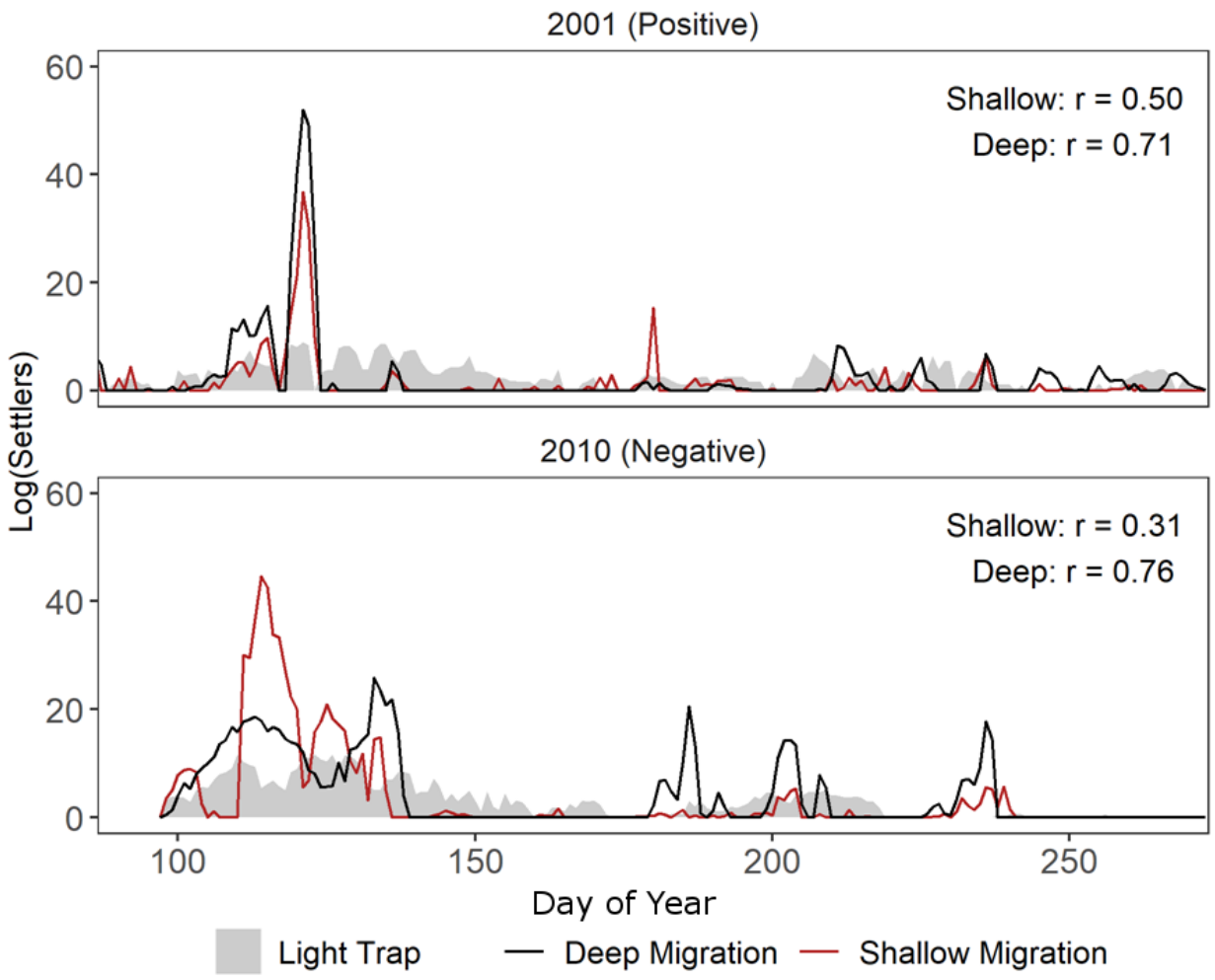

Fig. S7. Time series of megalopae return to a light trap in Coos Bay (shaded gray area) and settlers to the Coos Bay area in the shallow (red) and deep (black) simulations during 2001 (positive phase PDO year) and 2010 (negative phase PDO year; Table 1). In both years, the light trap catch was more strongly correlated with the deep than shallow simulations of larval migration.

The deep migration simulation was more strongly correlated with the light trap data than the shallow migration simulation (Table S1, Fig. S7). The relationship between larval release site and larval settlement site was examined using connectivity matrices (Fig. S8) where the nodes on the x-axis denotes the location simulated-larvae were released and the nodes on the y-axis denote the location where larvae settled. Settlement values are averages between years based on their corresponding PDO phase and ranged from 10^{15}-10^{25}. Overall, the deep migration simulations resulted in more settlement than the shallow migration simulations (Fig. S8). In the shallow migration simulations, more settlement occurred at the northern and southern extent of the model domain. Relatively little settlement occurred in the middle of the model domain. Further, there were especially few settlement events near ~ 43 °N, an area with a large and well established population of Dungeness crabs (Demory & others 1990). Thus, for the remainder of the paper we focus only on the deep migration simulations.

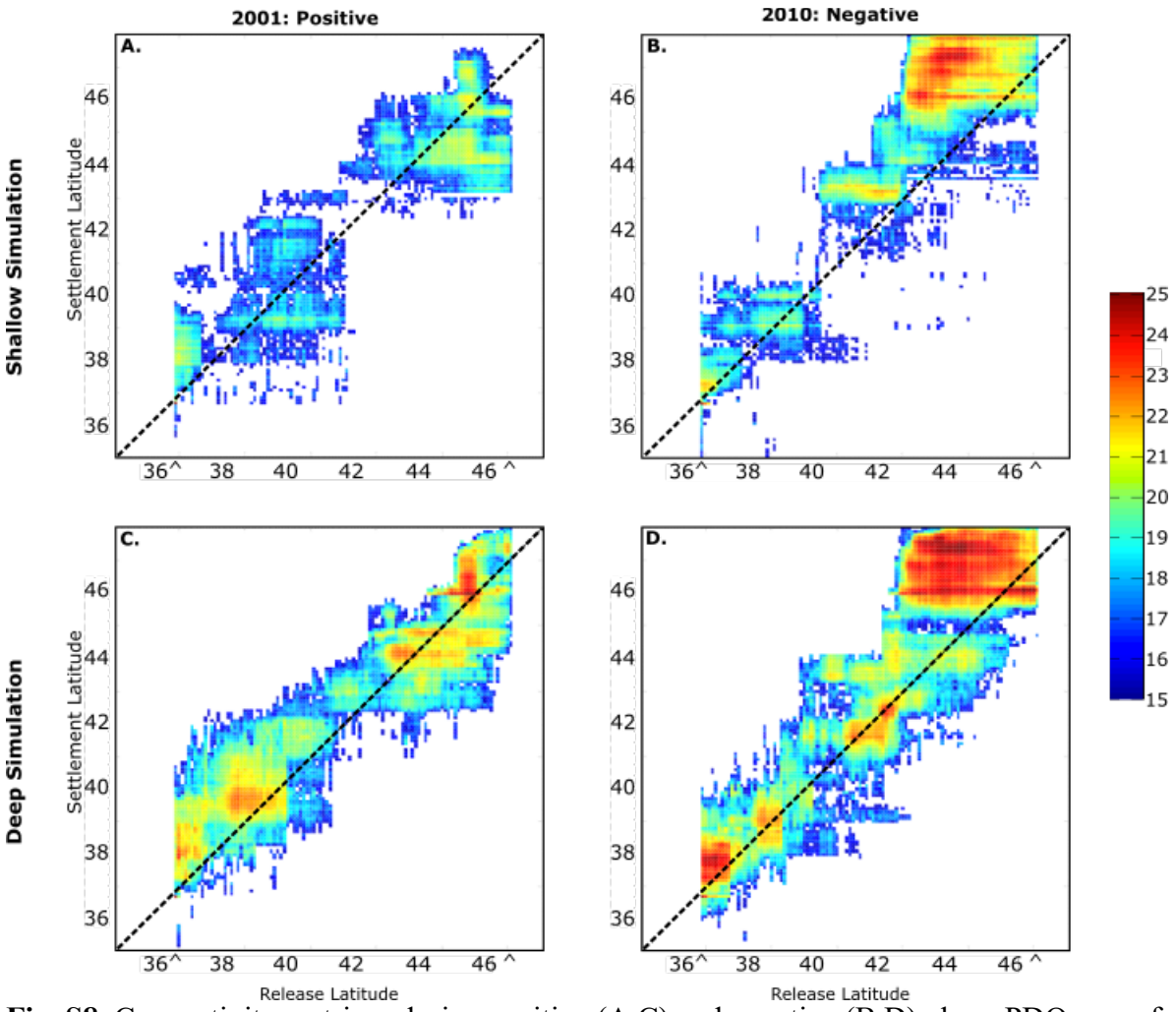

Fig. S8. Connectivity matrices during positive (A,C) and negative (B,D) phase PDO years for the shallow (A, B) and deep simulations (C,D). Nodes on x-axis denote where a larva was released and nodes on the y-axis denotes where a larva settled. Each node represents an average of all years in the corresponding PDO phase. The carrots on the x-axis denote the southern and northern extent of larval release. The dashed line is a 1:1 line, particles (model larvae) on the line settled where they were released, particles above and below the line ended up north and below south of where they were released. Scale bars denote $\log_{10}$ larvae.

Literature Cited

Botsford LW, Wickham DE (1978) Behavior of age-specific, density-dependent models and the northern California Dungeness crab (*Cancer magister*) fishery. J Fish Board Can 35:833–843.

Cowen RK, Lwiza KM, Sponaugle S, Paris CB, Olson DB (2000) Connectivity of marine populations: open or closed? Science 287:857–859.

Demory D, others (1990) History and status of the Oregon Dungeness crab fishery. Newport, Or.: Oregon Dept. of Fish and Wildlife, Marine Region.

Dunn PH, Shanks A (2012) Mating success of female Dungeness crabs (*Cancer magister*) in Oregon coastal waters. J Shellfish Res 31:1–5.

Gaumer T (1971) Closing report: controlled rearing of Dungeness crab larvae and the influence of environmental conditions on their survival. US Dep Inter Fish Wildl Serv Contract 14-17-0001-2325.

Hankin DG, Oh SJ (2004) The Sperm Plug Is a Reliable Indicator of Mating Success in Female Dungeness Crabs, *Cancer Magister*. J Crustac Biol 24:314–326.

Hobbs R, Botsford L (1992) Diel vertical migration and timing of metamophosis of larval Dungeness crab *Cancer magister.* Mar Biol 112:417–428.

Jamieson GS, Phillips A (1988) Occurence of Cancer crab (*C. magister and C. oregonensis*) megalopae off the west coast of Vancouver Island, British Columbia. Fish Bull 86:525–542.

McKelvey R, Hankin D, Yanosko K, Snygg C (1980) Stable cycles in multistage recruitment models: an application to the northern California Dungeness crab (*Cancer magister*) fishery. Can J Fish Aquat Sci 37:2323–2345.

Rasmuson L, Shanks A (2014) In situ observations of Dungeness crab megalopae used to estimate transport distances by internal waves. Mar Ecol Prog Ser 511:143–152.

Rasmuson LK (2013) The biology, ecology and fishery of the Dungeness crab, *Cancer magister*. Adv Mar Biol 65:95–148.

Rasmuson LK (2015) The influence of behavior and hydrodynamics on the dispersal of dungeness crab, *Cancer magister*, larvae. University of Oregon

Reilly P (1983) Dynamics of Dungeness crab, *Cancer magister*, larvae off central and northern California. Cal Dept Fish Game Fish Bull 172:57–84.

Rothlisberg PC, Pearcy WG (1976) An epibenthic sampler used to study the ontogeny of vertical migration of *Pandalus jordani*. Fish Bull 74:9–17.

Rumrill S (1990) Natural mortality of marine invertebrate larvae. Ophelia.

Shanks A, Roegner G, Miller J (2010) Using megalopae abundance to predict future commercial catches of Dungeness crabs (*Cancer magister*) in Oregon. CalCOFI Rep 51.

Shanks AL (2013) Atmospheric forcing drives recruitment variation in the Dungeness crab (*Cancer magister*), revisited. Fish Ocean 22:263–272.

Shanks AL, Roegner GC (2007) Recruitment limitation in Dungeness crab populations is driven by variation in atmospheric forcing. Ecology 88:1726–1737.